

ScaleNAS: One-Shot Learning of Scale-Aware Representations for Visual Recognition

Hsin-Pai Cheng^{1,2*}, Feng Liang^{1*}, Meng Li², Bowen Cheng³, Feng Yan⁴,
Hai Li¹, Vikas Chandra² and Yiran Chen¹

¹Duke University, ²Facebook Inc, ³University of Illinois at Urbana-Champaign, ⁴ University of Nevada, Reno

Abstract

Scale variance among different sizes of body parts and objects is a challenging problem for visual recognition tasks. Existing works usually design a dedicated backbone or apply Neural architecture Search(NAS) for each task to tackle this challenge. However, existing works impose significant limitations on the design or search space. To solve these problems, we present ScaleNAS, a one-shot learning method for exploring scale-aware representations. ScaleNAS solves multiple tasks at a time by searching multi-scale feature aggregation. ScaleNAS adopts a flexible search space that allows an arbitrary number of blocks and cross-scale feature fusions. To cope with the high search cost incurred by the flexible space, ScaleNAS employs one-shot learning for multi-scale supernet driven by grouped sampling and evolutionary search. Without further retraining, ScaleNet can be directly deployed for different visual recognition tasks with superior performance. We use ScaleNAS to create high-resolution models for two different tasks, ScaleNet-P for human pose estimation and ScaleNet-S for semantic segmentation. ScaleNet-P and ScaleNet-S outperform existing manually crafted and NAS-based methods in both tasks. When applying ScaleNet-P to bottom-up human pose estimation, it surpasses the state-of-the-art HigherHRNet. In particular, ScaleNet-P4 achieves 71.6% AP on COCO test-dev, achieving new state-of-the-art result.

1. Introduction

Deep-learned representation can be generally categorized into low-resolution representation and high-resolution representation. Low-resolution representation is typically used in classification tasks while high-resolution representation is essential for visual recognition tasks such as semantic segmentation and human pose estimation. We focus on the high-resolution representation in this paper. There are three important yet challenging considerations when

*equal contributions.

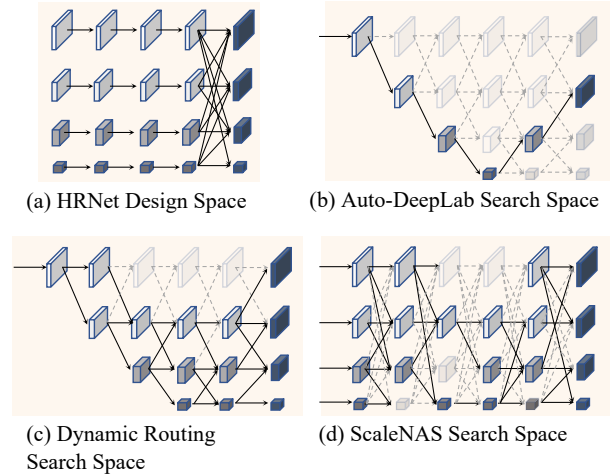


Figure 1. Search space comparison. (a) HRNet uses fully connected multi-scale feature fusion at the end of every four blocks. (b,c) Auto-DeepLab and dynamic routing allows feature fusion connection for each neighboring feature map and find the best architectures with single-path and multi-path, respectively. (d) We propose a more flexible feature fusion that allows crossing to remote feature maps to maximize multi-scale aggregation.

designing high-resolution representation: 1) scale variance from different sizes of objects and scenes; 2) precise and informative feature maps are critical; 3) different deployment platforms have different model size requirements.

Challenge of scale variance: take semantic segmentation as an example, the variance of object size induces difficulty for pixel-level dense prediction, and thus scale representation is critical. In human pose estimation, it is challenging to localize human anatomical keypoints when there is a large scale variance in the scene such as tiny and large persons, the large difference in joint distance. We address this challenge by proposing a new multi-scale search space.

Challenge of high-resolution representation: to design high-resolution representations, earlier efforts recover high-resolution representations from low-resolution outputs, e.g., Hourglass [24], SegNet [2], U-Net [28]. Recent

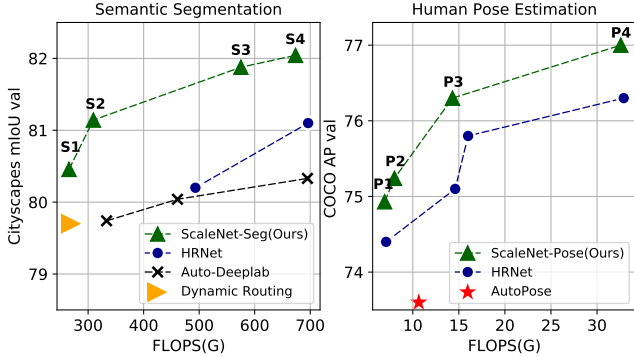


Figure 2. The trade-off between computation cost (GFLOPs) and model performance. Left: semantic segmentation mIoU on Cityscapes val. Right: human pose estimation AP on COCO val. Our ScaleNet outperforms HRNet and NAS-based methods.

works focus on maintaining high-resolution representation through the whole network and aggregating different scale of representation from parallel paths. E.g., HRNet [29, 30] and its variants use such multi-scale high-resolution networks to achieve state-of-the-art results on human pose estimation. However, multi-scale neural architectures usually have a large design space to explore and are prone to design redundancies. Our study reveals that when different scales of representation have different depths, the performance can be greatly improved.

Challenge of deriving a wide spectrum of models: previous methods can only derive one architecture at a time. To obtain different sizes of model, further retraining is required for each candidate architecture, e.g., it takes $O(N)$ training time to derive N models. We propose one-shot based searching method to lower the training cost to $O(1)$.

To address the above challenges, we propose ScaleNAS, a one-shot based searching method to explore scale-aware neural architectures. We tackle the scale variance challenge by proposing *multi-scale aggregation search space* to explore multi-scale aggregation and network depth for high-resolution representation, see Figure 1. Under this search space, we propose a one-shot based searching method to discover multiple architectures simultaneously.

We name these elite architectures ScaleNet, which can be directly deployed without retraining while performing as well as stand-alone models. As demonstrated in Figure 2, ScaleNet outperforms manually crafted and NAS-based models on semantic segmentation and human pose estimation. In semantic segmentation, ScaleNet surpasses HRNet, Auto-DeepLab, and dynamic routing by 1.3% - 1.7% mIoU on CityScapes dataset with less computation cost. In human pose estimation, our ScaleNet-P4 obtains 71.6% AP on COCO *test-dev2017*, achieving a new state-of-the-art result on multi-person pose estimation leaderboard. We further study the patterns of ScaleNet by analyzing the trade-offs between convolution blocks and feature

fusion for multi-scale neural architecture design.

2. Related Work

High-Resolution Neural Architectures. Designing high-resolution neural architectures is important yet challenging. For example, Hourglass [24] uses a high-to-low followed by a low-to-high architecture to achieve high-resolution. SimpleBaseline [31] uses transposed convolution layers to generate high-resolution representations. To prevent information loss from the encoding-decoding process, HRNet [30] proposed to keep high-resolution features at all times and use multi-scale feature fusion at the end of every four residual blocks to merge information from different scales. While this method has proven successful in many vision tasks, such manual design has many redundant operations and is not optimal as we demonstrated in Figure 3.

NAS for High-resolution Architectures. Recent works proposed automating the design of neural architectures for semantic segmentation and human pose estimation. For example, Auto-DeepLab and dynamic routing [17] are proposed to search architectures for semantic segmentation models. PoseNAS [3], AutoPose [12] and PNFS [32] are proposed to search architectures for human pose estimation.

However, the above NAS-based methods can only craft architectures for one task at a time. Given different platforms have different deployment constraints, previous works used adjustable factors (e.g., channel width) to scale neural architecture to different sizes [30]. After scaling, it is required to retrain each of the scaled architecture. Therefore, to get N models, it requires $O(N)$ training time. Since this procedure is costly and time consuming, we proposed a one-shot based searching method that can derive N models in $O(1)$ time without any retraining.

One-shot Neural Architecture Search. One-shot NAS aims at searching a large neural architecture and sharing weights to different sub-networks [26, 4, 21, 6, 13]. While these weights have to adapt to different sub-networks, one-shot NAS suffers from low accuracy. Recent works applied various techniques to conquer the low accuracy problem of supernet. For example, BigNAS [34] transforms the problem of training supernet to training a big single-stage model and applies sandwich rule to guarantee the performance for each sub-network. OFA [5] proposed to use progressive shrinkage together with knowledge distillation to train a one-shot supernet. However, these methods are mainly designed for single-path neural architecture on relatively simple task (e.g., ImageNet classification). Directly applying existing one-shot training methods to multi-scale architecture yields sub-optimal performance. In this paper, we solve this problem by our proposed *grouped sampling method* to effectively explore a wide spectrum of sub-networks and further search elite architectures with our evolutionary method.

3. ScaleNAS

In this section, we first identify the search space problems in existing works by performing a search space exploration. Then we introduce our proposed *multi-scale aggregation search space*. Based on this search space, we train a *one-shot based SuperScaleNet* that contains a wide spectrum of architecture candidates. Finally, we employ *multi-scale topology evolution* to derive elite ScaleNet based on a trained SuperScaleNet.

3.1. Search Space Exploration

Existing works that achieve state-of-the-art results on semantic segmentation and human pose estimation impose limitations on the design space. As shown in Figure 1, HRNet supports cross-scale feature fusions, but it uses four residual blocks in every scale of branches. Such regular design results in redundancy and misses optimization opportunities as the depth for each branch can be altered to improve performance.

Auto-DeepLab [20] includes multiple scale options in their search space to search a single-path neural architecture for semantic segmentation. Dynamic routing [17] reused the search space from Auto-DeepLab to search a multi-path neural architecture to achieve improved performance on semantic segmentation. Although Auto-DeepLab and dynamic routing search the connections between different scales of feature maps, the search space for fusion is limited to only neighboring scales. Such limitation restricts the representation ability for feature maps and cross-scale feature fusion can provide better information gathering for each scale of feature maps.

To illustrate our search space, we compare the proposed search space with existing works in Figure 1. Different from existing works, we provide flexible depth (number of residual blocks) for each scale of branch. In addition, we allow feature fusion cross to any other scale of branches. We use this search space to randomly sample neural architectures as ScaleNet-G series (Figure 3) and train them on Cityscapes. Original HRNet has 108 residual blocks [15] and 62 feature fusions. Residual block is composed of two 3×3 convolutions. Multi-scale fusion includes downsampling and upsampling. For downsampling, we use strided 3×3 convolution with stride 2. For upsampling, we use bilinear upsampling followed by a 1×1 convolution for aligning the number of channels [30]. We create ScaleNet-G1 by using the same number of blocks as HRNet while using 12 less feature fusions with our proposed search space, we observe that there are some ScaleNet-G1 models perform better than HRNet while having less number of fusions. Therefore, the feature fusion position of HRNet may not be optimal as shown in Figure 3. Based on ScaleNet-G1, we create ScaleNet-G2 and ScaleNet-G3 by increasing the number of fusions to the expectation of 124 and 198, re-

spectively. We notice that more feature fusions comes with a higher mIoU and inevitable comes with higher FLOPs. To study the redundancy of number of blocks, we create G4 and G5 by decreasing number of blocks while keeping higher number of fusions. We observe that the mean accuracy of ScaleNet-G4, G5 are still higher than the original HRNet setting. Based on this observation, we envision that we can use neural architecture search to explore the trade-offs and relationships between blocks and fusion connection.

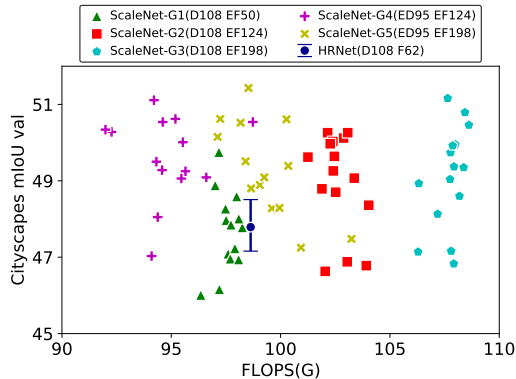


Figure 3. Search space exploration. We train HRNet five times and record the mean and variance of their accuracy. HRNet has 108 resblocks (denoted as ‘D’) and 62 fusions(denoted as ‘F’). We randomly sample 5 groups of ScaleNet with different resblocks and fusions based on our search space (Figure 1(d)). ‘ED’ and ‘EF’ represents the expectation of blocks and fusions, respectively.

3.2. Multi-scale Aggregation Search Space

Our goal is to design multi-scale neural architectures that can be adapted to multiple visual recognition tasks without retraining. Instead of searching a single model at a time, we aim at discovering a wide spectrum models that have different computation cost for different deployment scenarios.

We employ a stage-based search space design, which is inspired by the state-of-the-art architecture HRNet that can be adapted to multiple tasks. The architecture starts from a stem cell as the first stage and it is composed of two stride-2 3×3 convolutions. There are four stages in our search space. After the first stage, we gradually add one more high-to-low branch for the following stages, i.e., stage2, stage3, and stage4 maintains two-resolution, three-resolution, and four-resolution branches respectively.

Based on the initial experiments shown in Figure 3, we observe that fusion percentages has positive correlation with accuracy. Thus four blocks per branch proposed by HRNet is not always optimal. We introduce two Controlling factors to form our search space:

1. Branch depth (d). Instead of searching the overall depth for the entire network, we allow a more flexible search space that can search depth for each branch

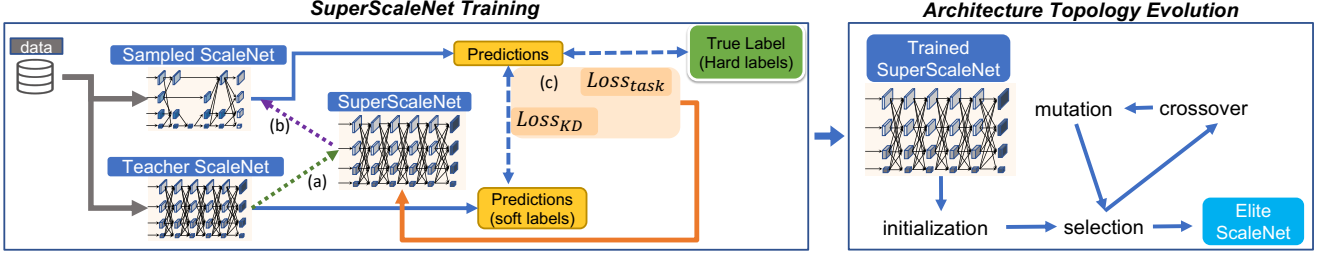


Figure 4. Workflow of ScaleNAS. ScaleNAS train a SuperScaleNet in the proposed search space and uses our proposed evolutionary method to explore elite architectures based on the trained SuperScaleNet. (a) Before training starts, we initialize SuperScaleNet by the teacher model. (b) During each iteration, we sample ScaleNet from the SuperScaleNet. (c) We use the task loss from true labels and the knowledge distillation (KD) loss from soft labels given by teacher to update SuperScaleNet.

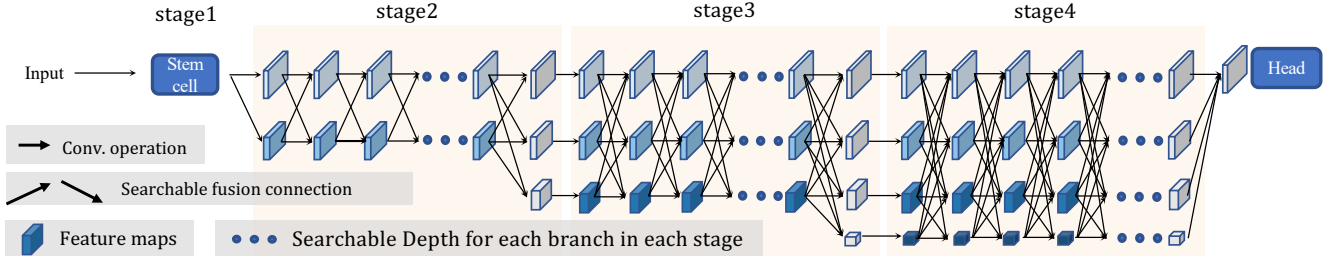


Figure 5. Search space overview of ScaleNAS. Our search space inherit the spirit of HRNet that has few stages. ScaleNAS adopts a flexible search space with arbitrary number of blocks and cross-scale feature fusions.

in individual independent stage module. For simplicity, the depth of each branch is chosen from $\{d1, d2, d3, d4\}$. In this paper, we currently set it at $\{2, 3, 4, 5\}$

2. Fusion percentage (f). Here the fusion percentage is defined as the probability of the out-degree fusion for each feature map. E.g., a feature map with fusion percentage of 100% means this feature map connects to every other scales of fusion in its current depth.

By relaxing the cross-scale feature fusion and enlarging the branch blocks, we have roughly 7×10^{72} different neural network architectures in our search space.

3.3. Training one-shot SuperScaleNet

In this section, we explain how to design a one-shot training for multi-scale aggregation search space. Recall that cross-scale feature fusion can boost up performance (see Figure 3). Here we propose to jointly train SuperScaleNet together with a teacher model that has sufficient feature fusion connection.

Figure 4 depicts the workflow of SuperScaleNet training. First, according to the search space proposed in Figure 5, we build the teacher model with full number of blocks and fully activated feature fusions. Visual recognition tasks usually rely on ImageNet pretrained to stabilize training [30, 27], we pretrain the teacher model on ImageNet until converge. Then, we initialize SuperScaleNet with the weights from the teacher model. During each

training iteration, we sample a sub-network from SuperScaleNet, pass one batch of training data to both sampled sub-network and teacher model. Next, we calculate the task loss using the true label, and knowledge distillation (KD) loss using the soft label given by teacher model. Finally, we update the supernet based on the combination of both task loss and KD loss. Our training objective is fomulated as follow:

$$\min_{W_s} \sum_{arch_i} (\mathcal{L}_{task}(P_{arch_i}, y) + \alpha \cdot MSE(P_{arch_i}, P_t)). \quad (1)$$

Our main goal is to optimize the weights of SuperScaleNet W_s with the combination of true label loss and soft label loss. Here P_{arch_i} stands for the prediction for each sampled architecture, y is the true label. P_t stands for the prediction from teacher model. We use MSE to calculate the loss between sub-network prediction and teacher network prediction. The KD ratio (α) is set to 1.

3.4. Grouped Sampling

To train supernet, sampling plays a crucial role. Sandwich rule [33, 34] was proposed to train supernet, where the smallest model, the largest model, and 2 randomly sampled models are trained in every iteration. However, we observe that sandwich rule cannot guarantee to explore a wide spectrum of neural architectures. Therefore, we propose grouped sampling by dividing the whole search space into different sub-groups.

Given a depth choice of $\{d1, d2, d3, d4\}$, we group the depth choice to $\{\{d1, d2\}, \{d2, d3\}, \{d3, d4\}\}$ (e.g., $\{[2, 3], [3, 4], [4, 5]\}$), the fusion percentage is selected from $\{f1, f2, f3\}$ (e.g., $\{0.2, 0.5, 0.8\}$). In combination, we have a total of 9 (3×3) sub-groups. Compared with sandwich rule, grouped sampling is more suitable for multi-scale aggregation search space. Empirical justification is detailed in Section 4.3.

It is worth noting that unlike in OFA [5] or BigNAS [34], where 4 sub-networks are sampled and their gradients are aggregated in each update step, our group sampling only get one sub-network in each iteration. Therefore, the cost of training a SuperScaleNet using group sampling is very low, e.g., equivalent to a standard model training.

3.5. Multi-scale Architecture Topology Evolution

To explore sub-network from a trained supernet, existing one-shot based methods use coarse-to-fine selection, predictor-based method, etc. However, these methods are mainly designed for single-path neural architecture. In comparison, our search space includes multiple path in each stage and each stage has different number of scales. Therefore, we propose *multi-scale architecture topology evolution*, which provides more reasonable and controllable crossover and mutation over candidate architectures.

As described in Algorithm 1 and Figure 4, our topology evolution include the following four phases.

- **Step1 Initialization.** We uniformly sample n_0 sub-networks and record their architectures, accuracies, and FLOPs as a set \mathbf{D} . n_0 equals to 1,000 in our experiments.
- **Step2 Selection.** We select top k models on the Pareto front of cost/accuracy trade-off curve in \mathbf{D} as candidate group \mathbf{C} . For each subnetwork in \mathbf{C} , we do crossover and mutation to obtain next-generation offsprings. k is set to 100 in our experiments.
- **Step3 Crossover.** Since different stage module may have different number of branches, our crossover is inner-stage crossover. For each sub-network arch_c in \mathbf{C} , we allow a probability p_c to swap stage module settings with another randomly selected sub-network. There are 8 stage modules (1,4,3 for stage 2, 3, 4, respectively) and p_c is set to 0.25. Thus, each sub-network is expected to have 2 modules been replaced.
- **Step4 Mutation.** After crossover, we do random mutation to switch on and off the fusion connections in every stage module with probability p_m . p_m is set to 0.5. These K offspring models along with their corresponding accuracies and FLOPs are recorded as set \mathbf{M} . Then we update $\mathbf{D} = \mathbf{D} \cup \mathbf{M}$. We continue to

Step2 until we have N sub-networks in \mathbf{D} . Here we set N as 2,000.

Algorithm 1 Multi-Scale Architecture Evolution

Input: Search space S , Trained SuperScaleNet, initial population size n_0 , number of offspring k , crossover probability p_c , mutation probability p_m , number of final elite architectures N .

Output: N Elite ScaleNet

- 1: Sample n_0 sub-networks to obtain initial population $\mathbf{D} = \{\text{arch}_d, d = 1, 2, 3, \dots, n_0\}$
 - 2: **while** $\text{len}(\mathbf{D}) < N$ **do**
 - 3: Select top k models on the Pareto front as candidate group $\mathbf{C} = \{\text{arch}_c, c = 1, 2, 3, \dots, k\}$
 - 4: **for** every sub-networks arch_c in \mathbf{C} **do**
 - 5: crossover and mutation under probability p_c and p_m sequentially, generate offspring
 - 6: Gather k offspring models as set $\mathbf{M}_k = \{\text{arch}_m, m = 1, 2, \dots, k\}$
 - 7: update $\mathbf{D} = \mathbf{D} \cup \mathbf{M}$
-

4. Experiments

In this section, we evaluate ScaleNAS by searching neural architectures for semantic segmentation and human pose estimation. First we train SuperScaleNet on semantic segmentation with Cityscapes dataset [10] and derive ScaleNet-S using ScaleNAS. Then we apply the same searching routine on top-down human pose estimation framework with COCO dataset [18] to derive ScaleNet-P. In order to evaluate the generalizability of ScaleNet, we apply ScaleNet-P to HigherHRNet framework for bottom-up human pose estimation. Finally, we conduct ablation studies for ScaleNAS.

Training setup. To stabilize training, we first train the teacher model with full depths and fusions on ImageNet-1k [11] dataset. Following the training procedure in [30], we train teacher model for 100 epochs. More training details can be found in the supplementary material.

4.1. Semantic Segmentation

Cityscapes. The Cityscapes [10] is a widely used dataset for semantic segmentation tasks, which contains 5,000 high quality pixel-level finely annotated scene images. The dataset is divided into 2975/500/1525 images for training, validation, and testing, respectively. There are 30 classes, and 19 classes among them are used for evaluation. The mean of class-wise intersection over union (*mIoU*) is adopted as our evaluation metric.

Implementation details. We first obtain the teacher model following the same training protocol in [36, 30]. The teacher model is trained for 484 epochs with the batch

Table 1. Semantic segmentation results on Cityscapes *val* (single scale and no flipping). The GFLOPs is calculated on the input size 1024×2048 . ‘D-X’ equals to ‘Dilated-X’. For existing segmentation NAS works, the total cost grows linear to the number of deployment scenarios N , while the cost of our ScaleNAS remains constant.

Method	Backbone	#Params	GFLOPs	mIoU (%)	Searching Cost (GPU hours)	Training Cost (GPU hours)	Total Cost($N=40$) (GPU hours)
DeepLabv3 [7]	D-ResNet-101	58.0M	1778.73	78.5	-	$50N$	-
DeepLabv3+ [8]	D-Xception-71	43.5M	1444.63	79.6	-	-	-
PSPNet [35]	D-ResNet-101	65.9M	2017.63	79.7	-	$100N$	-
Auto-DeepLab [20]	Searched-F20-ASPP	-	333.3	79.7	$72N$	$250N$	$12.9k$
Dynamic Routing [17]	Layer33-PSP	-	270.0	79.7	$180N$	0	$7.2k$
ScaleNAS (Ours)	ScaleNet-S1	25.3M	265.5	80.5	200	400	600
ScaleNAS (Ours)	ScaleNet-S2	28.5M	309.5	81.1	200	400	600
Auto-DeepLab [20]	Searched-F48-ASPP	-	695.0	80.3	$72N$	$350N$	$16.9k$
HRNet [30]	HRNet-W48	65.8M	696.2	81.1	-	$260N$	-
ScaleNAS (Ours)	ScaleNet-S4	67.5M	673.6	82.0	300	600	900

size of 24. After the teacher model is trained, we use our grouped sampling technique (Section 3.4) to further fine tune the SuperScaleNet-Seg to support smaller sub-networks. More training details can be found in the supplementary material.

Segmentation results. Table 1 reports the comparison between ScaleNAS and existing manual/NAS methods on semantic segmentation. Comparing with NAS (Auto-DeepLab and dynamic routing), ScaleNAS is much more efficient for multiple deployment scenarios. E.g., when there are 40 deployment scenarios, the total cost of ScaleNAS is $12\times$ fewer than dynamic routing and $19\times$ fewer than Auto-DeepLab, respectively. Without additional retraining, ScaleNet-S1 outperforms the dynamic routing Layer33-PSP by a 0.8% margin under the similar cost. When comparing with manually designed HRNet-W48 or Searched-F48-ASPP, ScaleNet-S4 improves the mIoU to 82.0%, surpassing HRNet and Auto-DeepLab by 0.9% and 1.7% respectively.

4.2. Human Pose Estimation

For human pose estimation, we first search ScaleNet-P on top-down human pose estimation task using COCO [18]. Then we reuse the searched ScaleNet-Pose on MPII [1] and bottom-up pose estimation tasks.

COCO. We train SuperScaleNet-Pose on COCO *train2017* dataset (57K images and 150K person instances) and evaluate it on COCO *val2017*. To evaluate object keypoints, we use Object Keypoint Similarity (OKS). We break down the performance on different OKS: AP_{50} and AP_{75} . We also report the performance on different sizes of object. AP_M and AP_L stands for AP of medium object and large object, respectively.

MPII. The MPII Human Pose dataset [1] consists real-world full-body pose and annotations. There are around 25K images with 40K subjects, where 12K subjects are used for testing and the remaining subjects are used for training. We use the PCKh (head-normalized probability of correct keypoint) score as our evaluation metric, following [31, 29]

4.2.1 Top-down Methods

Implementation details. We use the same workflow as semantic segmentation. Following the settings of [29, 30], the teacher model and SuperScaleNet-Pose are trained for 210 epochs. More training details can be found in the supplementary material.

Top-down results. Table 2 summarizes the results of top-down methods on COCO *val2017* and MPII *val*, compared with other state-of-the-art methods. Under 256×192 input resolution, our ScaleNet-P2 outperforms manually designed SimpleBaseline [31](+3.2%) and NAS based Auto-Pose [12](+1.6%) by a large margin. In addition, ScaleNet-P2 is comparable with the strong HRNet [30] baseline but with only 56% parameters and 55% FLOPs. With 384×288 input resolution, our ScaleNet-P3 achieves 76.3% AP on COCO *val2017*, outperforming PoseNFS-3 [32] by 3.3% AP with less computation cost. ScaleNet-P3 has the same accuracy as HRNet-W48 but uses only 42% parameters and 43% FLOPs. ScaleNet-P4 obtains 77.0% AP, surpassing its strong HRNet counterpart by 0.7% AP. For MPII, ScaleNet-P1 performs better on every body parts comparing with SimpleBaseline and HRNet.

4.2.2 Bottom-up Methods

We plug the elite architectures obtained from top-down human pose estimation into state-of-the-art bottom-up human estimation framework HigherHRNet [9].

Implementation details. We adopt the standard training procedure on COCO *train2017* as in [23, 9] and report results on COCO *val2017* and *test-dev2017*. The models are trained for 300 epochs. More training details can be found in the supplementary material.

Bottom-up results. Table 3 reports the results of bottom-up methods on COCO *val2017* and *test-dev2017*. By utilizing our ScaleNet-P as feature extractor, we boost the performance of bottom-up pose estimation. Our ScaleNet-P4

Table 2. Top-down human pose estimation results.

Comparison on COCO <i>val2017</i> . AutoPose* reports results without ImageNet pretraining.										
Method	Backbone	Input size	#Params	GFLOPs	AP	AP ₅₀	AP ₇₅	AP _M	AP _L	AR
SimpleBaseline [31]	ResNet-152	256×192	68.6M	15.7	72.0	89.3	79.8	68.7	78.9	77.8
AutoPose [12]	AutoPose*		-	10.65	73.6	90.6	80.1	69.8	79.7	78.1
HRNet [30]	HRNet-W48		63.6M	14.6	75.1	90.6	82.2	71.5	81.8	80.4
ScaleNAS (Ours)	ScaleNet-P2		35.6M	8.0	75.2	90.4	82.4	71.6	81.9	80.4
PNFS [32]	PoseNFS-3	384×288	-	14.8	73.0	-	-	-	-	-
SimpleBaseline [31]	ResNet-152		68.6M	35.6	74.3	89.6	81.1	70.5	79.7	79.7
HRNet [30]	HRNet-W48		63.6M	32.9	76.3	90.8	82.9	72.3	83.4	81.2
ScaleNAS (Ours)	ScaleNet-P3		26.2M	14.3	76.3	90.7	82.9	72.5	83.3	81.3
ScaleNAS (Ours)	ScaleNet-P4		64.3M	32.6	77.0	90.9	83.6	73.0	84.2	81.8
Comparison on MPII <i>val</i> . The GFLOPs is calculated on the input size 256 × 256. We reuse the searched ScaleNet-P and apply it to MPII dataset.										
Method	Backbone	#Params	GFLOPs	mean	Head	Shoulder	Elbow	Wrist	Hip	Knee
SimpleBaseline [31]	ResNet-152	68.6M	20.9	88.5	96.4	95.3	89.0	83.2	88.4	84.0
HRNet [30]	HRNet-W32	28.5M	9.5	90.3	97.1	95.9	90.3	86.4	89.1	87.1
ScaleNAS (Ours)	ScaleNet-P1	28.5M	9.3	91.0	97.3	96.5	91.5	87.3	90.0	87.5

Table 3. Bottom-up human pose estimation results.

Comparison on COCO <i>val2017</i> w/o multi-scale test.					
Method	Backbone	Input size	#Params	GFLOPs	AP
HigherHRNet [9]	HRNet-W32	512	28.6M	47.9	67.1
	ScaleNet-P1(Ours)	512	28.6M	46.9	67.8
	HRNet-W48	640	63.8M	154.3	69.9
	ScaleNet-P4(Ours)	640	64.4M	141.5	70.4
Comparison on COCO <i>test-dev 2017</i> w/ multi-scale test.					
Method	Backbone	Input size	#Params	GFLOPs	AP
Hourglass [23]	Hourglass	512	277.8M	206.9	63.0
Hourglass w/ refine [23]	Hourglass	512	277.8M	206.9	65.5
PersonLab [25]	ResNet-152	1401	68.7M	405.5	68.7
HigherHRNet [9]	HRNet-W48	640	63.8M	154.3	70.5
ScaleNAS (ours)	ScaleNet-P4(Ours)	640	64.4M	141.5	71.6

and ScaleNet-P1 outperform their counterparts by 0.7% AP and 0.5% AP on COCO *val2017*, respectively. In particular, our ScaleNet-P4 obtains 71.6% AP on COCO *test-dev2017* without using refinement or other post-processing techniques, achieving a new state-of-the-art result on multi-person pose estimation leaderboard.

4.3. Ablation Study

We perform ablation study on each proposed technique. All results are conducted with SuperScaleNet-Seg-W32 on Cityscapes. For simplicity, we denote SuperScaleNet-Seg-W32 as supernet in this part.

Impact of sampling. To study the impact of sampling technique, we train two supernet: one is based on our proposed method (Section 3.4), the other is based on state-of-the-art sampling method – sandwich rule [34]. We derive the Pareto front from these two supernet based on our proposed evolutionary search. In Figure 6, we show elite architectures and their corresponding accuracy from 220G to 320G. The Pareto front results suggest grouped sampling perform the best for multi-scale aggregation search space

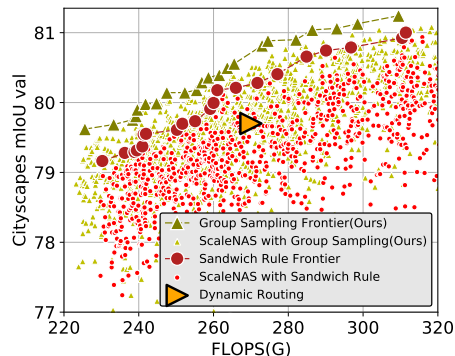


Figure 6. Ablation study of sampling techniques. The Pareto front of grouped sampling steadily higher than the Pareto front achieved by sandwich rule.

which has a wide spectrum of architectures.

Impact of topology evolution. We demonstrate the performance contribution from searching method by comparing with random search. We use random sampling to sample the same amount of architectures as our evolutionary method and plot the Pareto front. As shown in Figure 7, under the same searching budget, our multi-scale topology evolution consistently achieves better performance on Pareto front, thanks to our inner-stage crossover and mutation techniques.

Impact of knowledge distillation. We further study whether knowledge distillation (KD) plays an important role in accuracy gain. Based on the same training procedure in Section 4.1, we train ScaleNet-S1 from ImageNet pretrained weights (stand-alone) with and without KD. We use MSE loss with KD ratio 1 and the teacher model pretrained on Cityscapes. As shown in Table 4, the accuracy of the stand-alone training is only slightly lower than directly taken from supernet. It suggests that KD is beneficial but not a dominant factor in the final accuracy.

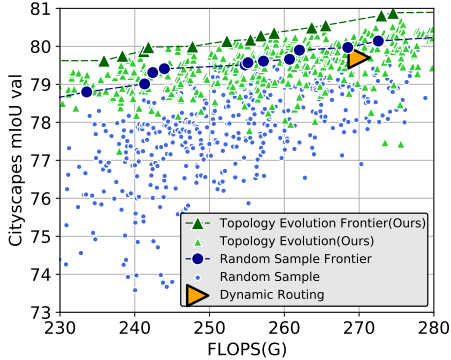


Figure 7. Ablation study of topology evolution. Dynamic routing is at around the Pareto curve of random sampling. The Pareto front of grouped sampling consistently higher than random sampling and dynamic routing.

Table 4. Ablation study of knowledge distillation (KD). Comparison with stand-alone training with and without KD. The performance mIoU(%) is obtained on Cityscapes *val*.

Model	from supernet	stand-alone w/o KD	stand-alone w/ KD
ScaleNet-S1	80.5	80.2	80.4

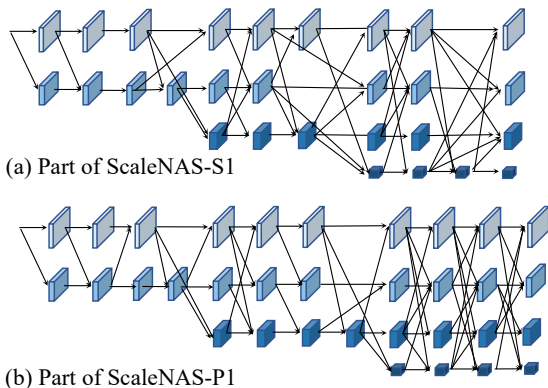


Figure 8. Architecture demonstration for ScaleNet-S1 and ScaleNet-P1.

5. Discussion

Crafted architectures. We demonstrate the crafted architectures for both semantic segmentation and human pose estimation in Figure 8. We show the first module for each stage (full model description is in supplementary material). We observe that both architectures have various cross-scale feature fusion, which is important for handling large scale variance in these tasks. In addition, we observe later stages rely on heavier feature fusions while earlier stages have less feature fusions.

Elite architecture pattern analysis. Different hardware platforms have different computation constraints. We analyze the deployability of elite architectures with different computation cost. We record FLOPs, the number of fusions,

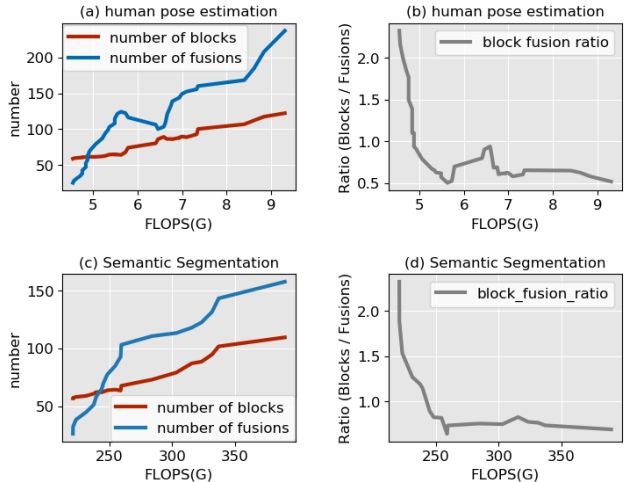


Figure 9. The network pattern of elite sub-networks. We show the relationship between number of blocks and fusions for the elite sub-networks.

and the number of blocks of Pareto front from the 2000 elite ScaleNets collected by our evolutionary method.

In Figure 9(a)(c), we observe larger elite models have more fusions than blocks. In addition, the number of fusions increases faster than the number of blocks. To further analyze the relationship between number of fusions and number of blocks, we demonstrate block-fusion ratio in Figure 9(b)(d). We observe that for the largest elite model, it requires two times more fusions than blocks. However, for small elite models, the number of fusions is only half of the number of blocks. This interesting observation provides important future design insights: 1) For edge devices, we should invest more computation cost on blocks than fusions. 2) To design larger models, it is preferable to invest computation cost on fusions over blocks.

6. Conclusion

We present ScaleNAS, a one-shot learning method for scale-aware representations. To the best of our knowledge, ScaleNAS is the first of its kind one-shot NAS method that considers scale variance for multiple vision recognition tasks. To efficiently search a wide spectrum of neural architectures for different vision tasks, we rest upon the following key ideas: (i) A novel multi-scale feature aggregation search space that includes cross scale feature fusions and flexible depths. (ii) One-shot based training method driven by an efficient sampling technique to train multi-scale supernet. (iii) Multi-scale architecture topology evolution to efficiently search elite neural architectures. All the above novel ideas coherently make ScaleNAS outperform existing hand crafted and NAS-based methods on semantic segmentation and human pose estimation.

References

- [1] Mykhaylo Andriluka, Leonid Pishchulin, Peter Gehler, and Bernt Schiele. 2d human pose estimation: New benchmark and state of the art analysis. In *Proceedings of the IEEE Conference on Computer Vision and Pattern Recognition*, pages 3686–3693, 2014. 6
- [2] Vijay Badrinarayanan, Alex Kendall, and Roberto Cipolla. Segnet: A deep convolutional encoder-decoder architecture for image segmentation. *IEEE transactions on pattern analysis and machine intelligence*, 39(12):2481–2495, 2017. 1
- [3] Qian Bao, Wu Liu, Jun Hong, Lingyu Duan, and Tao Mei. Pose-native network architecture search for multi-person human pose estimation. In *Proceedings of the 28th ACM International Conference on Multimedia*, pages 592–600, 2020. 2
- [4] Gabriel Bender, Pieter-Jan Kindermans, Barret Zoph, Vijay Vasudevan, and Quoc Le. Understanding and simplifying one-shot architecture search. In *International Conference on Machine Learning*, pages 550–559, 2018. 2
- [5] Han Cai, Chuang Gan, Tianzhe Wang, Zhekai Zhang, and Song Han. Once for all: Train one network and specialize it for efficient deployment. In *International Conference on Learning Representations*, 2020. 2, 5
- [6] Han Cai, Ligeng Zhu, and Song Han. Proxylessnas: Direct neural architecture search on target task and hardware. *arXiv preprint arXiv:1812.00332*, 2018. 2
- [7] Liang-Chieh Chen, George Papandreou, Florian Schroff, and Hartwig Adam. Rethinking atrous convolution for semantic image segmentation. *arXiv preprint arXiv:1706.05587*, 2017. 6
- [8] Liang-Chieh Chen, Yukun Zhu, George Papandreou, Florian Schroff, and Hartwig Adam. Encoder-decoder with atrous separable convolution for semantic image segmentation. In *Proceedings of the European conference on computer vision (ECCV)*, pages 801–818, 2018. 6
- [9] Bowen Cheng, Bin Xiao, Jingdong Wang, Honghui Shi, Thomas S Huang, and Lei Zhang. Higherhrnet: Scale-aware representation learning for bottom-up human pose estimation. In *Proceedings of the IEEE/CVF Conference on Computer Vision and Pattern Recognition*, pages 5386–5395, 2020. 6, 7, 11
- [10] Marius Cordts, Mohamed Omran, Sebastian Ramos, Timo Rehfeld, Markus Enzweiler, Rodrigo Benenson, Uwe Franke, Stefan Roth, and Bernt Schiele. The cityscapes dataset for semantic urban scene understanding. In *Proceedings of the IEEE conference on computer vision and pattern recognition*, pages 3213–3223, 2016. 5
- [11] Jia Deng, Wei Dong, Richard Socher, Li-Jia Li, Kai Li, and Li Fei-Fei. Imagenet: A large-scale hierarchical image database. In *2009 IEEE conference on computer vision and pattern recognition*, pages 248–255. Ieee, 2009. 5
- [12] Xinyu Gong, Wuyang Chen, Yifan Jiang, Ye Yuan, Xianming Liu, Qian Zhang, Yuan Li, and Zhangyang Wang. Autopose: Searching multi-scale branch aggregation for pose estimation. *arXiv preprint arXiv:2008.07018*, 2020. 2, 6, 7, 11
- [13] Zichao Guo, Xiangyu Zhang, Haoyuan Mu, Wen Heng, Zechun Liu, Yichen Wei, and Jian Sun. Single path one-shot neural architecture search with uniform sampling. In *European Conference on Computer Vision*, pages 544–560. Springer, 2020. 2
- [14] Kaiming He, Georgia Gkioxari, Piotr Dollár, and Ross Girshick. Mask r-cnn. In *Proceedings of the IEEE international conference on computer vision*, pages 2961–2969, 2017. 11
- [15] Kaiming He, Xiangyu Zhang, Shaoqing Ren, and Jian Sun. Deep residual learning for image recognition. In *Proceedings of the IEEE conference on computer vision and pattern recognition*, pages 770–778, 2016. 3
- [16] Diederik P Kingma and Jimmy Ba. Adam: A method for stochastic optimization. *arXiv preprint arXiv:1412.6980*, 2014. 10, 11
- [17] Yanwei Li, Lin Song, Yukang Chen, Zeming Li, Xiangyu Zhang, Xingang Wang, and Jian Sun. Learning dynamic routing for semantic segmentation. In *Proceedings of the IEEE/CVF Conference on Computer Vision and Pattern Recognition*, pages 8553–8562, 2020. 2, 3, 6, 11
- [18] Tsung-Yi Lin, Michael Maire, Serge Belongie, James Hays, Pietro Perona, Deva Ramanan, Piotr Dollár, and C Lawrence Zitnick. Microsoft coco: Common objects in context. In *European conference on computer vision*, pages 740–755. Springer, 2014. 5, 6
- [19] Marius Lindauer and Frank Hutter. Best practices for scientific research on neural architecture search. *arXiv preprint arXiv:1909.02453*, 2019. 11
- [20] Chenxi Liu, Liang-Chieh Chen, Florian Schroff, Hartwig Adam, Wei Hua, Alan L Yuille, and Li Fei-Fei. Auto-deeplab: Hierarchical neural architecture search for semantic image segmentation. In *Proceedings of the IEEE conference on computer vision and pattern recognition*, pages 82–92, 2019. 3, 6
- [21] Hanxiao Liu, Karen Simonyan, and Yiming Yang. Darts: Differentiable architecture search. *arXiv preprint arXiv:1806.09055*, 2018. 2
- [22] Ilya Loshchilov and Frank Hutter. Sgdr: Stochastic gradient descent with warm restarts. *arXiv preprint arXiv:1608.03983*, 2016. 10
- [23] Alejandro Newell, Zhiao Huang, and Jia Deng. Associative embedding: End-to-end learning for joint detection and grouping. In *Advances in neural information processing systems*, pages 2277–2287, 2017. 6, 7
- [24] Alejandro Newell, Kaiyu Yang, and Jia Deng. Stacked hour-glass networks for human pose estimation. In *European conference on computer vision*, pages 483–499. Springer, 2016. 1, 2
- [25] George Papandreou, Tyler Zhu, Liang-Chieh Chen, Spyros Gidaris, Jonathan Tompson, and Kevin Murphy. Personlab: Person pose estimation and instance segmentation with a bottom-up, part-based, geometric embedding model. In *Proceedings of the European Conference on Computer Vision (ECCV)*, pages 269–286, 2018. 7
- [26] Hieu Pham, Melody Y Guan, Barret Zoph, Quoc V Le, and Jeff Dean. Efficient neural architecture search via parameter sharing. *arXiv preprint arXiv:1802.03268*, 2018. 2

- [27] Shaoqing Ren, Kaiming He, Ross Girshick, and Jian Sun. Faster r-cnn: Towards real-time object detection with region proposal networks. In *Advances in neural information processing systems*, pages 91–99, 2015. 4, 11
- [28] Olaf Ronneberger, Philipp Fischer, and Thomas Brox. U-net: Convolutional networks for biomedical image segmentation. In *International Conference on Medical image computing and computer-assisted intervention*, pages 234–241. Springer, 2015. 1
- [29] Ke Sun, Bin Xiao, Dong Liu, and Jingdong Wang. Deep high-resolution representation learning for human pose estimation. In *Proceedings of the IEEE conference on computer vision and pattern recognition*, pages 5693–5703, 2019. 2, 6, 11
- [30] Jingdong Wang, Ke Sun, Tianheng Cheng, Borui Jiang, Chaorui Deng, Yang Zhao, Dong Liu, Yadong Mu, Mingkui Tan, Xinggang Wang, et al. Deep high-resolution representation learning for visual recognition. *IEEE transactions on pattern analysis and machine intelligence*, 2020. 2, 3, 4, 5, 6, 7, 10
- [31] Bin Xiao, Haiping Wu, and Yichen Wei. Simple baselines for human pose estimation and tracking. In *Proceedings of the European conference on computer vision (ECCV)*, pages 466–481, 2018. 2, 6, 7, 10, 11
- [32] Sen Yang, Wankou Yang, and Zhen Cui. Pose neural fabrics search. *arXiv preprint arXiv:1909.07068*, 2019. 2, 6, 7
- [33] Jiahui Yu and Thomas S Huang. Universally slimmable networks and improved training techniques. In *Proceedings of the IEEE International Conference on Computer Vision*, pages 1803–1811, 2019. 4
- [34] Jiahui Yu, Pengchong Jin, Hanxiao Liu, Gabriel Bender, Pieter-Jan Kindermans, Mingxing Tan, Thomas Huang, Xi-aodan Song, Ruoming Pang, and Quoc Le. Bignas: Scaling up neural architecture search with big single-stage models. *arXiv preprint arXiv:2003.11142*, 2020. 2, 4, 5, 7
- [35] Hengshuang Zhao, Jianping Shi, Xiaojuan Qi, Xiaogang Wang, and Jiaya Jia. Pyramid scene parsing network. In *Proceedings of the IEEE conference on computer vision and pattern recognition*, pages 2881–2890, 2017. 6
- [36] Hengshuang Zhao, Yi Zhang, Shu Liu, Jianping Shi, Chen Change Loy, Dahua Lin, and Jiaya Jia. Psanet: Point-wise spatial attention network for scene parsing. In *Proceedings of the European Conference on Computer Vision (ECCV)*, pages 267–283, 2018. 5

7. Supplementary Material

This supplementary material provides more details of training SuperScaleNet on each task and also the extension of object detection task. For *reproducibility*, **we provide full searching and training codes, as well as pretrained models**. Please refer to README.md to see detailed instructions.

7.1. Details of Search Space Exploration

In our main submission, we conduct initial search space exploration on semantic segmentation using Cityscapes. All

models are trained from scratch for 48 epochs. Data augmentation strategies and other training protocols are the same as the teacher training part of Section 7.3 in this supplementary material.

7.2. Details of Training Teacher Model on ImageNet

Following the instructions in [30], we use stochastic gradient descent (SGD) as the optimizer with 0.9 nesterov momentum and 0.0001 weight decay. The model is trained for 100 epochs with batch size 768. The initial learning rate is set to 0.3 and is reduced by 10 at epoch 30, 60, and 90. It takes ~ 30 hours to train on 16 TESLA V100 GPUs.

7.3. Details of Training SuperScaleNet on Semantic Segmentation

Teacher training: For a fair comparison, we follow the same training protocols in [30]. We adopt the SGD optimizer with the momentum of 0.9 and the weight decay of 0.0005. The model is trained for 484 epochs with the batch size of 24 on 8 TESLA V100 GPUs. The initial learning rate is set to 0.01 and the cosine annual decay [22] is used for decaying the learning rate. For data preprocessing, the training and validation image size is 512×1024 and 1024×2048 , respectively. For data augmentation strategies, we use random cropping (from 1024×2048 to 512×1024), random scaling (between [0.5, 2]), and random horizontal flipping.

SuperScaleNet-Seg training: We follow the same training protocols as teacher training except the initial learning rate is set to 0.001. This is because the SuperScaleNet-Seg is initialized from the well-trained teacher, we only need to fine-tune each sub-network using a small learning rate.

It takes $\sim 40(60)$ hours to obtain SuperScaleNet-Seg-W32(W48), including the teacher training. With only twice the training cost as stand-alone model training, we can obtain a series of segmentation models in a wide spectrum of FLOPs without additional retraining. We further use multi-scale topology evolution to explore elite ScaleNet-Seg.

7.4. Details of Training SuperScaleNet on Top-Down Human Pose Estimation

Teacher training: Following the training protocols of HRNet [30], we train the model for 210 epochs using the Adam optimizer [16] with step learning rate decay [31, 30]. The initial learning rate is set as 0.001, and is dropped to 0.0001 and 0.00001 at the 170th and 200th epochs, respectively. For data preprocessing, we extend the human detection box in height or width to a fixed aspect ratio – height : width = 4 : 3, and then crop the box from the image, which is resized to a fixed size, 256×192 or 384×288 . For data augmentation strategies, we use random rotation ($[-45^\circ, 45^\circ]$), random scale ([0.65, 1.35]), and flipping.

Table 5. Object detection results on COCO *minival* in Faster R-CNN [27] and Mask R-CNN [14]. LS denotes learning rate scheduler. GFLOPs is calculated on the input size 800×1280. HRNet-w32* denotes our reimplementation.

Backbone	LS	Params(M)	GFLOPs	box				mask			
				AP	AP _S	AP _M	AP _L	AP	AP _S	AP _M	AP _L
Faster R-CNN [27]											
HRNet-w32*	1×	47.2	285.4	39.8	22.8	43.7	51.0	/	/	/	/
ScaleNet-S2	1×	46.3	271.3	40.1	23.9	44.2	51.7	/	/	/	/
Mask R-CNN [14]											
HRNet-w32*	1×	49.9	353.9	40.8	23.8	44.5	52.4	36.4	19.5	39.7	48.9
ScaleNet-S2	1×	49.0	339.8	40.9	24.4	44.6	52.5	36.5	19.7	40.0	49.0

SuperScaleNet-Pose training: We follow the same training protocols in teacher training. We do not reduce the learning rate as in SuperScaleNet-Seg training because the Adam optimizer can adjust the learning rate adaptively [16].

The models are trained on 8 TESLA V100 GPUs. It takes ~50(75) hours to train SuperScaleNet-Pose-W32(W48), including the teacher training. After topology evolution, we further fine-tune the ScaleNet-P for 20 epochs (around 3 hours) for better performance.

MPII: We use the same data augmentation and training strategy for MPII, except that the input size is cropped to 256 × 256 for a fair comparison with SimpleBaseline [31] and HRNet [29].

7.5. Details of Training found architectures on Bottom-Up Human Pose Estimation

We train ScaleNet-P series on bottom-up human pose estimation framework, HigherHRNet [9]. For a fair comparison, we use the exact same training routine as HigherHRNet. Specifically, we train our model for 300 epochs using the Adam optimizer [16] with step learning rate decay. The base learning rate is set to 0.001, and dropped to 1e-4 and 1e-5 at the 200th and 260th epochs, respectively. For data augmentation strategies, we use random rotation ([-30°, 30°]), random scale ([0.75, 1.5]), random translation ([-40, 40]), random crop (512 × 512), and random flip. We use the top-down SuperScaleNet-Pose to initialize weights.

7.6. Results on Object Detection

We directly apply the ScaleNet-S2, which is obtained from semantic segmentation, to object detection task. We plug in the ScaleNet-S2 to two classic object detection frameworks, Faster R-CNN [27] and Mask R-CNN [14] as shown in Table 5. We use the whole COCO *trainval135* as training set and validate on COCO *minival*. For both Faster R-CNN and Mask R-CNN, the input images are resized to a short side of 800 pixels and a long side not exceeding 1333 pixels. We use SGD as optimizer with 0.9 momentum. For a fair comparison, all our models are trained for 12 epochs, known as 1× scheduler. We use 8 TESLA V100 GPUs for training with 16 global batch size. The initial learning rate is 0.02 and is divided by 10 at 8 and 11 epochs.

In the Faster R-CNN framework, our networks perform better than HRNet-w32 with less parameters and computation cost. Our ScaleNet-S2 is especially effective for small objects (1.1% improvement for AP_S). The reason is that our ScaleNet-S2 learns more high-resolution features which are beneficial for small objects.

7.7. Details of Found Architecture

Here we provide the architecture structures of our crafted architecture ScaleNet-P1 for human pose estimation and ScaleNet-S1 for semantic segmentation, see Figure 10 and Figure 11, respectively. The interesting observation is that both architectures have more multi-scale feature fusion at later stages while with a relatively simple network structure at the early stages.

7.8. NAS Reproducibility Checklist

To ensure a fair comparison, we follow the guidelines provided by NAS reproducibility checklist [19] and compare ScaleNAS with other NAS methods from different perspectives.

✓ *For all NAS methods you compare, did you use exactly the same NAS benchmark, including the same dataset (with the same training-test split), search space and code for training the architectures and hyperparameters for that code?*

– For comparing with other NAS methods [12, 17], we used the same dataset including train-test split. Our search space is essentially different from previous works. To train our architecture, we used the open-sourced repository from HRNet and HigherHRNet with the only change of learning rate.

✓ *Did you control for confounding factors (different hardware, versions of DL libraries, different runtimes for the different methods)?*

– Yes, for the version of DL libraries, we used Pytorch-1.1 for conducting all our experiments

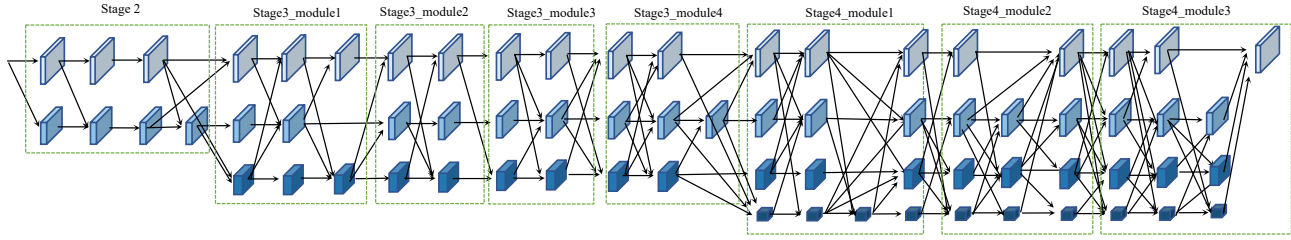


Figure 10. The full model of ScaleNet-S1.

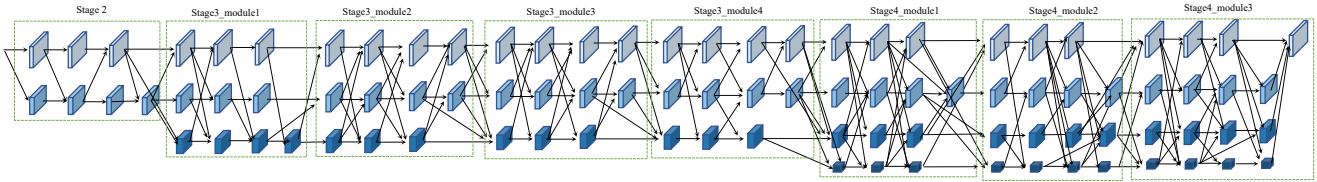


Figure 11. The full model of ScaleNet-P1.

and collecting our results. All the package dependencies are described in `requirements.txt` of our attached codes. For hardware, we only trained and tested on NVIDIA TESLA V100 GPU.

✓ *Did you run ablation studies?*

- Yes, we performed ablation studies for sampling method, searching method, and knowledge distillation. Detailed results can be found in Section 4.3 of our main submission.

✓ *Did you use the same evaluation protocol for the methods being compared?*

- Yes, for evaluating on top-down human pose estimation, we followed the same evaluation protocol as HRNet paper. For comparing with bottom-up human pose estimation, we used the same evaluation protocol as HigherHRNet. For comparing on semantic segmentation, we used the same evaluation protocol as HRNet as well.

✓ *Did you compare to random search?*

- Yes, we compared our searching method with random search at Section 4.3 and Figure 7 of our main submission. The results show that the Pareto front of our found architectures performs better than random search.

✓ *Did you perform multiple runs of your experiments?*

- Yes, during search space exploration, we trained the original HRNet 5 times and reported the mean and standard deviation of mIoU on

Cityscapes. For SuperScaleNet, we only trained once. We expect further tuning and training should achieve better results. All of our experiment is highly reproducible and source code is provided.

□ *Did you use tabular or surrogate benchmarks for in-depth evaluations?*

- No, existing surrogate benchmarks such as NASBench-101, NAS-Bench-201, NAS-Bench-1Shot1 are not application to our search space.

✓ *Did you report how you tuned hyperparameters, and what time and resources this required?*

- Yes, among all the hyperparameters, we only tuned the learning rate for training SuperScaleNet on semantic segmentation tasks. Since SuperScaleNet-Seg is initialized from the well-trained teacher, the original learning rate (0.01) used in HRNet is not suitable for our case. We tried three different learning rates, 0.005, 0.002, and 0.001. Each tuning cost 300 GPU hours, with a total cost of around 900 GPU hours on TESLA V100. We found that the learning rate of 0.001 shows the best performance, thus, we use 0.001 for semantic segmentation tasks.

✓ *Did you report all the details of your experimental setup?*

- Yes, we comprehensively reported all of the configurations, including hyperparameter settings, training protocol in main submission and supplementary material.